Results in Physics 10 (2018) 665–674

Contents lists available at ScienceDirect

Results in Physics

journal homepage: www.elsevier.com/locate/rinp

# Inhibition performance of *Glycine* max, *Cuscuta reflexa* and *Spirogyra* extracts for mild steel dissolution in acidic medium: Density functional theory and experimental studies

D.K. Verma[a], Fahmida Khan[b], I. Bahadur[c,d], Mohammad Salman[e], M.A. Quraishi[e,f], Chandrabhan Verma[c,d,*], Eno E. Ebenso[c,d,*]

[a] Department of Chemistry, Govt. Digvijay Autonomous Postgraduate College, Rajnandgaon, Chhattisgarh 491441, India
[b] Department of Chemistry, National Institute of Technology, Raipur, Chhattisgarh 492010, India
[c] Department of Chemistry, School of Chemical and Physical Sciences, Faculty of Natural and Agricultural Sciences, North-West University, Private Bag X2046, Mmabatho 2735, South Africa
[d] Material Science Innovation & Modelling (MaSIM) Research Focus Area, Faculty of Natural and Agricultural Sciences, North-West University, Private Bag X2046, Mmabatho 2735, South Africa
[e] Department of Chemistry, Indian Institute of Technology, Banaras Hindu University, Varanasi 221005, India
[f] Center of Research Excellence in Corrosion, Research Institute, King Fahd University of Petroleum & Minerals, Dhahran 31261, Saudi Arabia

ARTICLE INFO

*Keywords:*
Acid solution
Electrochemical studies
Adsorption
Mild steel
Green inhibitors
EDS-SEM

ABSTRACT

The effectiveness of three plant extracts namely *Glycine* max leaves (GMLE), *Cuscuta reflexa roxb.* (CRRE) and *Spirogyra* algae (SGAE) has been evaluated as green corrosion inhibitors for mild steel corrosion in acidic solution of 1 M HCl using chemical, electrochemical, surface and density functional theory (DFT) methods. The gravimetric and electrochemical results showed that the trend of their effectiveness towards mild steel acidic corrosion inhibition follows the order: GMLE > CRRE > SGAE. Polarization study suggested that tested plant extracts acted as mixed type inhibitors with slight anodic dominance. The GMLE, CRRE and SGAE extracts showed maximum inhibition efficiencies of 73.60%, 81.92% and 94.05%, respectively at 2 g $L^{-1}$ concentration. Results of gravimetric measurements showed that effectiveness of the plant extracts enhances on enhancing their concentrations. Gravimetric measurements carried out at different temperature showed that adsorption of the plant extracts mainly involve physisorption mechanism. Investigated extracts behaved as interface inhibitors and their adsorption mechanism obeyed the Langmuir adsorption isotherm. Surface morphology and elemental composition was determined to support the adsorption inhibitive mechanism. Scanning electron microscope (SEM) analyses carried out in the association with electron dispersive X-ray spectroscopy (EDS) further supported the adsorption inhibitive mechanism. Density Functional Theory (DFT) study was carried out on major phytochemicals present in the extract in order to support the experimental results and explain the adsorption behaviour of phytochemicals (extracts).

## Introduction

In various industries iron based alloys such as carbon steel and mild steel are widely used as manufacturing materials as they have very high mechanical strength and relative cheaper price. However, at the same time their uses are limited particularly in petroleum industries and during some industrial processes like oil-will acidification, pickling, acid de-scaling and industrial acid cleaning [1]. Cleaning industries mainly utilized aggressive acidic solutions of phosphoric acid ($H_3PO_4$), sulphuric acid ($H_2SO_4$) and most commonly hydrochloric acid (HCl) [2]. Although, use of the organic compounds is most common practice towards inhibition of metallic and alloys corrosion, however recently their use is limited because of their poisonous and non-environmental friendly properties. Organic inhibitors are generally toxic, harmful and associated with huge discharge of toxic chemicals and solvents after their synthesis and even after their use in corrosion monitoring. In this regard, the use of plant extracts as green corrosion inhibitors offer a widely employed alternative source of the metallic corrosion protection [3]. Generally, plant products are environmental friendly, renewable, bio-decomposable in nature, easily and economically available those

* Corresponding authors at: Department of Chemistry, School of Mathematical & Physical Sciences, Faculty of Agriculture, Science and Technology, North-West University (Mafikeng Campus), Private Bag X2046, Mmabatho 2735, South Africa.
*E-mail addresses:* chandraverma.rs.apc@itbhu.ac.in (C. Verma), Eno.Ebenso@nwu.ac.za (E.E. Ebenso).

https://doi.org/10.1016/j.rinp.2018.06.003
Received 15 May 2018; Received in revised form 31 May 2018; Accepted 2 June 2018
Available online 07 June 2018

make the one of the best suitable and alternative green source for corrosion inhibition. Nowadays, use of plant extracts as green and susceptible corrosion inhibitors has gained noteworthy development because of their environmentally benign, highly efficient and cost-effective nature [4]. The use of plant materials as inhibitors is growing interest of the scientist working in the field of corrosion science and technology because of their sustainable nature and presence of several phytochemicals that contain π- and non-bonding electrons for their effective adsorption and inhibition. Literature study suggests that previously extracts of several plant extracts such as foods, flowers, roots, stems and leaves etc. have been employed for effective inhibition of corrosion. The few common examples that have substantial corrosion protection ability towards protection of mild steel acidic ($H_3PO_4$, HCl, $H_2SO_4$) corrosion are extracts of *Bamboo leaves* [7], *Artemisia pallens* [5], *Mentha rotundifolia* [8], *Coconut coir* [6], *Musa paradisiac*, *Camellia sinensis* [9], *Zanthoxylum alatum extract*, *black pepper* and *Alstonia angustifolia* var. *latifolia*. Present study targets to evaluate the inhibition on ability of three plant extracts symbolized as CRRE, GMLE & SGAE on mild steel corrosion in the destructive acidic medium of 1 M HCl using commonly employed experimental methods such as weight loss, SEM-EDS and Electrochemical methods. *Bryophyllum Pinnatum* leaves used to treat kidney stones and gastric ulcers, and externally for lesions, boils, burns, ulcers, insect bites and eye infection [10]. Many activities such as antimicrobial [11] and antianaphylactic [12] studied extensively. Various phytochemical studies showed that the plant contained flavone, coumarin as major phytoconstituents along with alkaloids, tannins, phenols, flavonoids, glycosides, anthocyanins, bufadienolides, lectins and saponins [13–16]. Soybean plants are richly abundant in physically active metabolites such as isoflavones, tocopherols, polyphenol and saponin. There is a special interest in soybean isoflavone globally, because epidemiological studies have shown that their consumption may be linked to fewer incidences of cancer [17] and the risk of various diseases, including cardiovascular problems and symptoms of menopause [18] and diabetes mellitus type II [19]. The extract of soybean leaves contain several flavonoids such as daidzein, glycitein, and genistein etc. as main phytoconstituents [20].The long history of medicinal applications of *Cuscuta reflexa roxb* has inspired various pharmacological research work. Studies indicate that *Cuscuta reflexa roxb* shows a series of biological activities such as skin protective activity, immune regulation, antioxidant activity, antisenser activity, antimatozenic effects, antidiabetic activity, antidirippress activity, CNS depression and anti-inflammatory. [21]. Chemical components of *Cuscuta reflexa roxb are f*lavonoids, poly-saccharides, alkaloids, steroids and lignans, where quercetin, berginin (cuscutin) and Kaempferol are found in the form of active phytoconstituents [22].

## Experimental

### *Materials*

Surface (SEM and EDS), weight loss and electrochemical studies were carried on the metallic specimens that had chemical composition of: C (0.25%), O (0.06%), P (0.03%), Mn (0.46%), S (0.05%), Cr (0.49%) and Fe (98.66%). The different grades (400–1200) of emery papers were employed to abrade and clean the metallic specimens to be used in experiments. Double distilled water derived from Elix essential 10 millipore water distillator was used to dilute the purchased analytical grade HCl (37% HCl, MERCK) into 1 M HCl. Several concentrations of the tested plant extracts ranging from 0.5 to 2.0 g $L^{-1}$ used for gravimetric study, while the electrochemical and surface studies were carried out at 2.0 g $L^{-1}$ concentration (optimum concentration). Plant extracts were prepared according to the previously described standard procedure [34].

**Table 1**
Polarisation indices for dissolution of mild steel in 1 M HCl solution with optimum concentration of SGAE, CRRE and GMLE at 298 K.

| Inhibitors | Conc. of inhibitors (g $L^{-1}$) | Tafel polarisation parameters | | | | | |
|---|---|---|---|---|---|---|---|
| | | $I_{corr}$ | $E_{corr}$ | $\beta_a$ | $-\beta_c$ | $\theta$ | $\%\eta$ |
| | Blank | 84.28 | −517 | 656.2 | 121.4 | – | – |
| SGAE | 2.0 | 21.96 | −514 | 112.6 | 199.3 | 0.7394 | 73.94 |
| CRRE | 2.0 | 16.09 | −507 | 126.7 | 134.6 | 0.8090 | 80.90 |
| GMLE | 2.0 | 4.99 | −522 | 117.4 | 132.2 | 0.9407 | 94.07 |

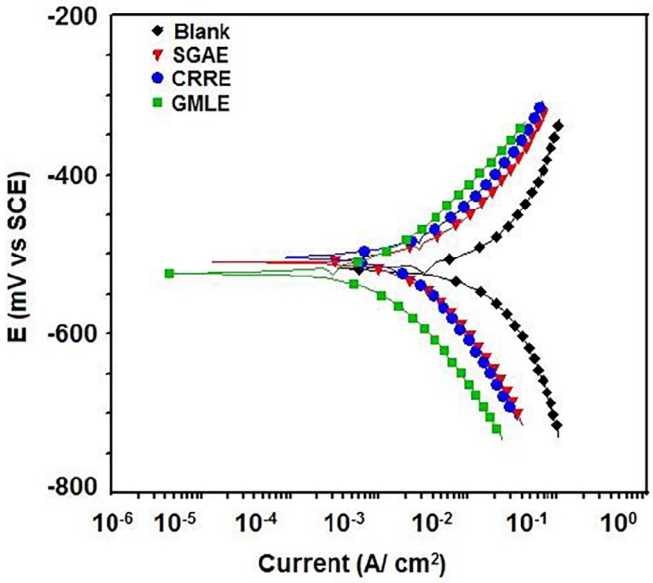


**Fig. 1.** Polarization curve for mild steel in 1 M HCl in the absence and optimum concentrations (2 g $L^{-1}$) of the plant extracts.

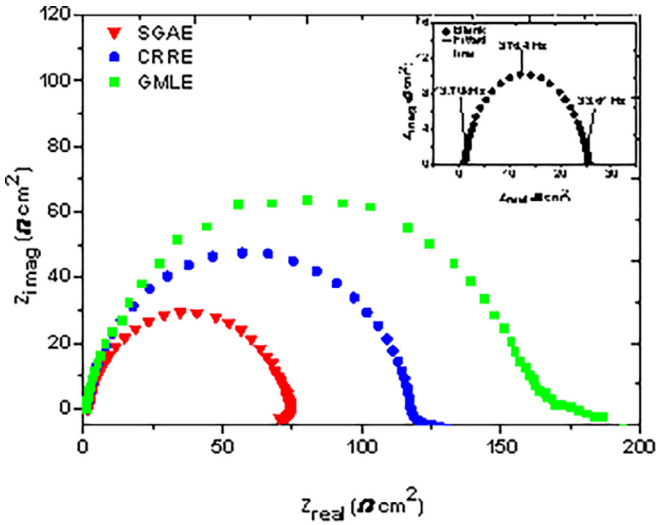


**Fig. 2.** Nyquist plots for mild steel in 1 M HCl in the absence and optimum concentrations (2 g $L^{-1}$) of the plant extracts.

### *Methods*

#### *Electrochemical measurement*

Electrochemical studies were accomplished at the optimum concentration of three investigated plant extracts using standard Potentiostat/Galvanostat instrument which contained three electrode assembly. In the present investigation, saturated calomel (SCE) was

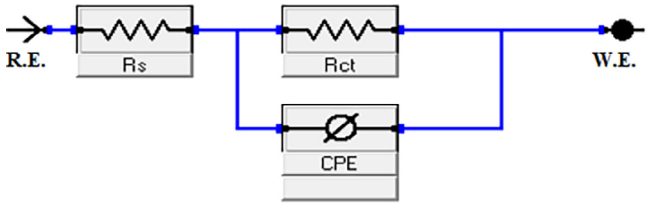


**Fig. 3.** Electrochemical equivalent circuit model used to fit the impedance spectra.

employed as reference or standard electrode, while pure platinum of specific size of 1 $cm^2$ was used as counter electrode and metallic specimen of 1 $cm^2$ was employed as working electrode. It is recall that electrochemical studies carried out at the optimum concentration of three studied plant extracts for mild steel in acid solution. The Gamry Potentiostat/Galvanostat instrument that have Model G-300 was taken for study the electrochemical behaviour of mild steel in acid solution in the presence of 1 M HCl solution. This instrument contains Echem Analyst (5.0 version) software through which electrochemical data were analysed and interpreted. The 30 min immersion of the working specimens in the test solution before performing the electrochemical studies allow the stabilization of OCP which stand open circuit potential necessary for electrochemical measurements. While performing impedance measurements for inhibited and uninhibited working electrodes, the frequency range of 100 kHz to 0.01 mHz and fixed amplitude value of 10 mV peak to peak were chosen.

The electrochemical measurements at every studied concentration of GMLE, CRRE and SGAE is triply performed in order to insure the reproducibility of the measurement. Presentation of inhibition efficiencies of tested plant extracts at their 2.0 g $L^{-1}$ concentration were calculated using Eq. (1) [27]:

$$\%\eta = \frac{R_{ct(inh)} - R_{ct}}{R_{ct(inh)}} \times 100 \quad (1)$$

In Eq. (1), $R_{ct(inh)}$ and $R_{ct}$ respectively represent the charge transfer resistances for inhibited and non-inhibited metallic specimens. For potentiodynamic polarization studies, working electrode potential is allowed the change from −250 to +250 V with respect to the potential of SCE at the constant scan rate of 1 mV $s^{-1}$ similar to our previous reports [2,27]. Following Eq. (2) was employed to calculate the efficiency from the values of current densities ($i_{corr}$) those are evaluated by extrapolating the cathodic and anodic linear segments of Tafel polarization curves [28]:

$$\%\eta = \frac{i_{corr} - i_{corr(inh)}}{i_{corr}} \text{x } 100 \quad (2)$$

In above equation, $i_{corr}$ and $i_{corr\ (inh),}$ respectively denote the current density values for uninhibited and inhibited metallic working electrodes.

*Gravimetric analysis*

Previous studies manifest that gravimetric analysis is an important, accurate and simple method for evaluation of protection ability of the inhibitors because of its association with accurateness and reliability along with simplicity and preciseness. Concentration of plant extracts ranging from 0.5 to 2.0 g $L^{-1}$ were used for gravimetric analysis for the 6 h of immersion period at studied temperatures (298–328 K). After completion of the weight loss experiment (6 h) working electrodes of mild steel removed from the inhibited and uninhabited systems, washed to remove the corrosion product using millipore (distilled) water, dried and weighted precisely using an electronic balance (METTLER TOLEDO) of high sensitivity (0.0001 g). The weight loss experimental at every studied concentration of GMLE, CRRE and SGAE is triply performed in order to insure the reproducibility of the measurement. The corrosion rate (ρ) of mild steel in acidic solution was calculated using the following relation [28]:

$$\rho = \frac{\Delta w}{At} \quad (3)$$

In Eq. (3), ΔW manifest the loss in the weight of working electrode (in mg), $A$ represents the total surface area of the working electrode (in $cm^2$) and $t$ represents the time (6 h). Percentage of efficiency ($\%\eta$) for studied plant extracts at their different concentrations were derived from the Eq. (4):

$$\%\eta = \left(\frac{\rho^1 - \rho^2}{\rho^1}\right) \times 100 \quad (4)$$

where $\rho^1$ and $\rho^2$ represent the corrosion rates of working electrodes with and without plant extracts, correspondingly.

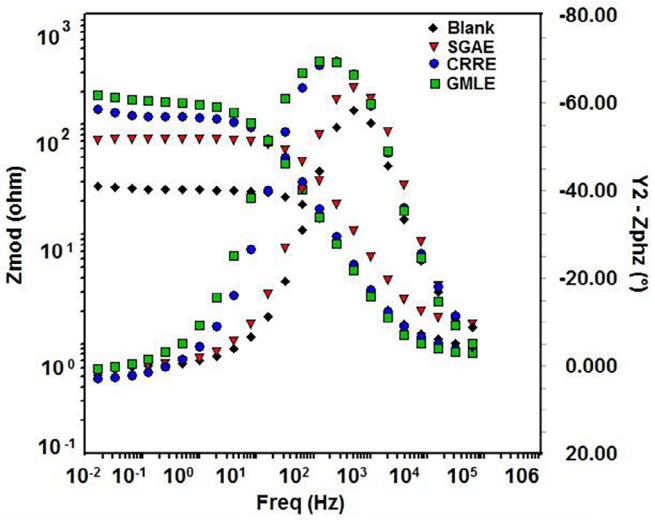


**Fig. 4.** Bode-phase plots of mild steel corrosion in 1 M HCl with and without inhibitors at room temperature.

*Surface analysis*

Mild steel (working electrode) specimens were dipped in the test solution of 1 M HCl in the absence and presence of 2.0 g $L^{-1}$ concentration of the tested plant extracts. The surface morphology of working electrode and change in elemental composition at working electrode surface were analysed after removing them from tested solution. For SEM and EDS investigations, ZEISS EVO SEM 18 model having INCA 250 EDS X-MAX 20 mm Detector Oxford was used.

**Table 2**
EIS parameters for mild steel corrosion in 1 M HCl in the absence and presence of optimum concentration of SGAE, CRRE and GMLE at 298 K at 298 K.

| Inhibitor | Conc. (g $L^{-1}$) | $R_s$ (Ω $cm^2$) | $R_{ct}$ (Ω $cm^2$) | $C_{dl}$ (μF $cm^{-2}$) | $\chi^2$ | $\theta$ | $\%\eta$ |
|---|---|---|---|---|---|---|---|
| | Blank | 0.991 | 23.31 | 122.4 | $1.42 \times 10^{-3}$ | – | |
| SGAE | 2.0 | 1.612 | 70.98 | 83.62 | $348.9 \times 10^{-6}$ | 0.661 | 67.15 |
| CRRE | 2.0 | 0.913 | 120.9 | 82.36 | $3.062 \times 10^{-3}$ | 0.800 | 80.71 |
| GMLE | 2.0 | 0.836 | 174.8 | 70.13 | $1.681 \times 10^{-3}$ | 0.860 | 86.66 |

**Table 3**
Parameters derived for SGAE, CRRE and GMLE from weight loss measurements at studied temperatures.

| Inhibitor (s) | Conc. ($g\,L^{-1}$) | Corrosion rate, ρ, ($mg\,cm^{-2}\,h^{-1}$) | | | | Inhibition Efficiency (%$\eta$) | | | |
|---|---|---|---|---|---|---|---|---|---|
| | | 298 K | 308 K | 318 K | 328 K | 298 K | 308 K | 318 K | 328 K |
| SGAE | 0.0 | 1.135 | 2.122 | 4.465 | 5.884 | – | – | – | – |
| | 0.5 | 0.297 | 0.549 | 1.258 | 1.786 | 73.83 | 74.12 | 71.82 | 69.64 |
| | 1.0 | 0.256 | 0.510 | 1.202 | 1.705 | 77.44 | 75.96 | 73.07 | 71.02 |
| | 1.5 | 0.213 | 0.484 | 1.176 | 1.689 | 81.23 | 77.19 | 73.66 | 71.29 |
| | 2.0 | 0.195 | 0.457 | 1.113 | 1.623 | **82.81** | 78.46 | 75.07 | 72.41 |
| CRRE | 0.0 | 1.022 | 1.988 | 4.223 | 5.631 | – | – | – | – |
| | 0.5 | 0.158 | 0.358 | 0.913 | 1.558 | 84.54 | 81.99 | 78.38 | 72.33 |
| | 1.0 | 0.133 | 0.309 | 0.886 | 1.497 | 86.98 | 84.45 | 79.01 | 73.41 |
| | 1.5 | 0.118 | 0.284 | 0.811 | 1.422 | 88.45 | 85.71 | 80.79 | 74.74 |
| | 2.0 | 0.097 | 0.255 | 0.769 | 1.386 | **90.50** | 87.17 | 81.79 | 75.38 |
| GMLE | 0.0 | 0.966 | 1.925 | 4.102 | 5.597 | – | – | – | – |
| | 0.5 | 0.159 | 0.334 | 0.788 | 1.244 | 83.54 | 82.64 | 80.78 | 77.77 |
| | 1.0 | 0.121 | 0.297 | 0.516 | 1.136 | 87.47 | 84.57 | 87.42 | 79.70 |
| | 1.5 | 0.102 | 0.243 | 0.482 | 0.987 | 89.44 | 87.37 | 88.24 | 82.36 |
| | 2.0 | 0.089 | 0.198 | 0.454 | 0.811 | **90.78** | 89.71 | 88.93 | 85.51 |

*Quantum chemical study*

DFT is being the most frequently utilized as computational techniques for the corroboration of experimental results and also to explain the adsorption behaviour of several organic compounds at the metallic surface. In view of this, in the present study DFT study has been performed on the major phytochemicals of the extracts. Using Gaussian 09 (G00) software package several DFT indices were computed using following relationships as described in literatures [2]:

$$IE = -E_{HOMO} \tag{5}$$

$$EA = -E_{LUMO} \tag{6}$$

$$\eta = \frac{1}{2}(IE{-}EA) = \frac{1}{2}(-E_{HOMO} + E_{LUMO}) \tag{7}$$

$$\sigma = \frac{1}{\eta} \tag{8}$$

$$\chi = \frac{1}{2}(IE + EA) = \frac{1}{2}(-E_{HOMO}{-}E_{LUMO}) \tag{9}$$

$$\Delta N = \frac{\chi_{Fe}{-}\chi_{inh}}{2(\eta_{Fe} + \eta_{inh})} \tag{10}$$

Because of the lowest energy of Fe (1 1 0) surface crystalline form of iron, we have employed 4.88 eV value as electronegativity of the iron in the present study for the calculation of value of fraction of electron transfer ($\Delta N_{110}$).

## Results and discussions

*Electrochemical investigations*

*Tafel polarization*

The mechanism of anodic dissolution and cathodic hydrogen evolution was investigated for mild steel in uninhibited and inhibited by plant extracts. Tafel polarization indices are presented in Table 1 inspection of which reveals that the values of current densities ($i_{corr}$) in the presence of $2.0\,g\,L^{-1}$ concentration of each plant extracts are much lower as compared to in the absence of plant extracts (blank solution). Uninhibited and inhibited by plant extracts Tafel polarization curves are presented in Fig. 1. These Tafel curves were plotted at room temperature for all studied plant extracts. Visualization of Tafel curves manifests that presence of GMLE, CRRE and SGAE at their optimum concentration affect the corrosive behaviour of anodic and cathodic curves. The linear segments of these curves were chosen and extrapolated to compute some common Tafel parameters namely current density ($i_{corr}$), corrosion potential ($E_{corr}$) and cathodic and anodic Tafel slopes ($\beta_c$, $\beta_a$) (Table 1). Results showed that tested plant extracts showed the maximum efficiencies of 73.60%, 81.90% and 94.05 for SGAE, CRRE, and GMLE, respectively at $2.0\,g\,L^{-1}$ concentration. Table 1 clearly shows that a significant decreased cathodic and anodic current density values was observed in the presence of $2.0\,g\,L^{-1}$ which is caused by adsorption of phytochemicals/ phyto-constituents over the metal (mild steel)-electrolyte (1M HCl) interfaces. Further, very minor shift ( ± 15 mV) in the value of *E*corr was observed for inhibited mild steel specimen as compared to uninhibited working electrode indicating the mixed type nature of all studied inhibitors (GMLE, CRRE AND SGAE) [29,36].

*EIS study*

The kinetics of working electrode corrosion in aggressive solution of 1 M HCl was studied using EIS method. The EIS measurements were carried out at the $2.0\,g\,L^{-1}$ concentration of the studied plant extracts. Fig. 2 demonstrate the Nyquist plots for uninhibited and inhibited by the plant extracts at room temperature that represent imperfect semicircles of different diameters. The corrosive dissolution of the working electrode in the test solution in both the cases involve charge transfer phenomenon as demonstrated by single semicircle in the Nyquist plots. Moreover, Careful visualization of the plots reveals that diameter of the curves increased significant in the presence of plant extracts and increase in their diameters follow their order of effectiveness. The increased diameters of Nyquist plots inhibited by plant extracts showed that charge transfer from metal to electrolyte (1M HCl) became difficult owing to formation of protective film by phytochemicals of the plant extracts. The EIS data were analysed employing most commonly used electrochemical circuit comprising of charge transfer resistance ($R_{ct}$), double layer capacitance ($C_{dl}$) and solution resistance ($R_s$) (Fig. 3). Table 2 showed the increased value *R*ct and decreased values of $C_{dl}$ for inhibited mild steel specimens by plant extracts in 1 M HCl which is attributed to the adsorption of phytochemical present in the plant extracts on the meta-solution interfaces [30,37]. Careful observation of the presented results showed that increase in *R*ct values and decrease in the $C_{dl}$ values obeyed the order of their effectiveness.

Fig. 4 represents the Bode impedance magnitude and phase angle plots for mild steel with and without inhibitors in 1 M HCl. In the Bode plots, phase angle at high frequencies provided a general idea of inhibition performance and working electrode surface roughness. It is well documented that lower phase angle values related with high surface roughness and vice versa. Formation of single constant or maxima in the Bode plots suggests that mild steel corrosion in 1 M HCL with and without plant extracts involves the single charge transfer mechanism. It

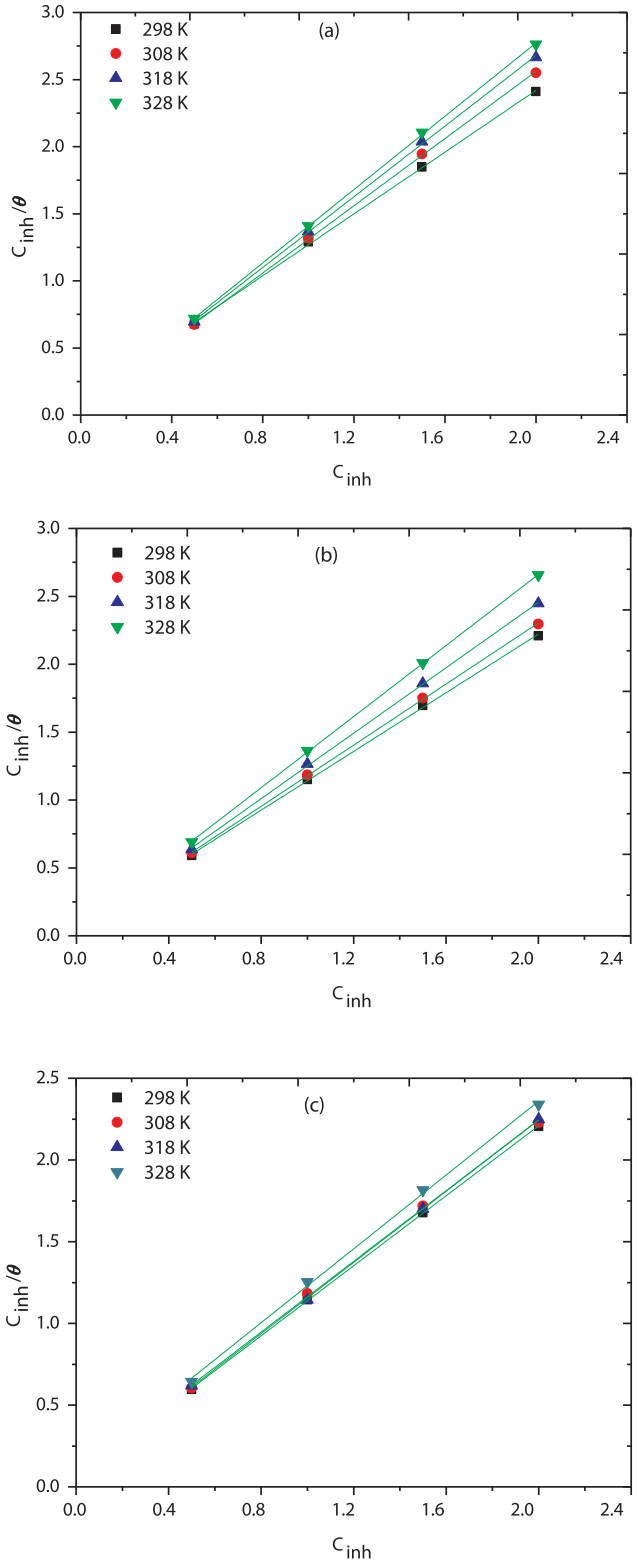


**Fig. 5.** Langmuir adsorption plot for mild steel in 1 M HCl in the presence of utilized corrosion inhibitors: (a) SGAE, (b) CRRE and (c) GMLE at different temperatures.

can be observed from the Bode plot that phase angle significantly increased in the presence of plant extracts due to the formation of the protecting film on the mild steel surface. This finding suggests that presence of plant extracts in the corrosive medium of 1 M HCl causes adsorption of the active phytochemicals that ultimately resulted into the decreased corrosive damaged of the surface and enhanced surface smoothness. The value of goodness of fit has been given in Table 2.

**Table 4**
Thermodynamic parameters derived for SGAE, CRRE and GMLE at studied temperatures.

| Inhibitor | Temp. (K) | $R^2$ | $K_{ads}$ (L g$^{-1}$) | $\Delta G_{ads}$ (kJ mol$^{-1}$) |
|---|---|---|---|---|
| SGAE | 298 | 0.999 | 08.54 | −15.26 |
| | 308 | 0.999 | 17.54 | −17.62 |
| | 318 | 0.999 | 21.27 | −18.70 |
| | 328 | 0.999 | 24.39 | −19.66 |
| CRRE | 298 | 0.999 | 16.26 | −16.86 |
| | 308 | 0.999 | 18.51 | −17.75 |
| | 318 | 0.999 | 21.27 | −18.70 |
| | 328 | 0.999 | 22.72 | −19.46 |
| GMLE | 298 | 0.999 | 14.81 | −16.62 |
| | 308 | 0.998 | 12.19 | −16.68 |
| | 318 | 0.999 | 15.15 | −17.80 |
| | 328 | 0.998 | 09.95 | −17.21 |

*Weight loss studies*

*Effect of concentration*

The inhibition efficiency of the plant extracts on corrosive behaviour of 1 M HCl for mild steel has also been demonstrated using weight loss experiments at 0.5, 1.0, 1.5 and 2.0 g L$^{-1}$ concentrations of each plant extracts. The derived parameters at different concentrations (0.5–2.0 g L$^{-1}$) and temperatures (298–328 K) are presented in Table 3. Observation of the results depicted in the Table 3 showed corrosion rate values decreases with increase in the plant extracts concentration and decrease in the temperature and vice versa. The maximum efficiencies of 82.81%, 90.50% and 90.78% were observed for SGAE, CRRE and GMLE, respectively at 2.0 g L$^{-1}$ concentration. The increased in plant extract concentration increases the surface coverage values which in turn enhances inhibition efficiency till the maximum surface coverage achieved. After 2.0 g L$^{-1}$ concentration corrosion inhibition efficiency of plant extracts did not varied substantially. As the solution temperature increases, kinetic energy of the phytochemicals increases in the same order that result into decrease in the attraction between phytochemicals and metals surfaces and ultimately inhibition performance [23,24,31,38]. At elevated temperatures, the high rate of decomposition and desorption of phytochemicals from the metallic surface is also attribute in the reduction of inhibition efficiency i.e. at higher solution temperature equilibrium for adsorption-desorption processes shifted in the direction of desorption phenomenon [35].

*Adsorption isotherm*

The surface coverage ($\theta$) values of three plant extracts derived at their studied concentrations (0.5–2.0 g L$^{-1}$) were plotted together in order to derive best adsorption isotherm and mechanistic/ mode of adsorption. In the present study, we tried to fit several common isotherms such as Temkin, freundlich and Langmuir adsorption isotherm among that best fit was obtained in case of Langmuir adsorption isotherm for tested plant extracts in which values of regression coefficient were most close to unity. Generally, Langmuir adsorption isotherm is resulted due to monolayer adsorption of the active phytochemicals present over the metallic surface. It is important to mention that generally in most of the metal-inhibitor interaction processes, phytochemicals or organic inhibitors initially interact by physisorption (multilayer) mechanism and finally chemisorption (monolayer) mechanism. The relationship between surface coverage ($\theta$) and the plant extracts concentrations ($C$) following Langmuir equation [32]:

$$\frac{C}{\theta} = \frac{1}{K_{ads}} + C \tag{11}$$

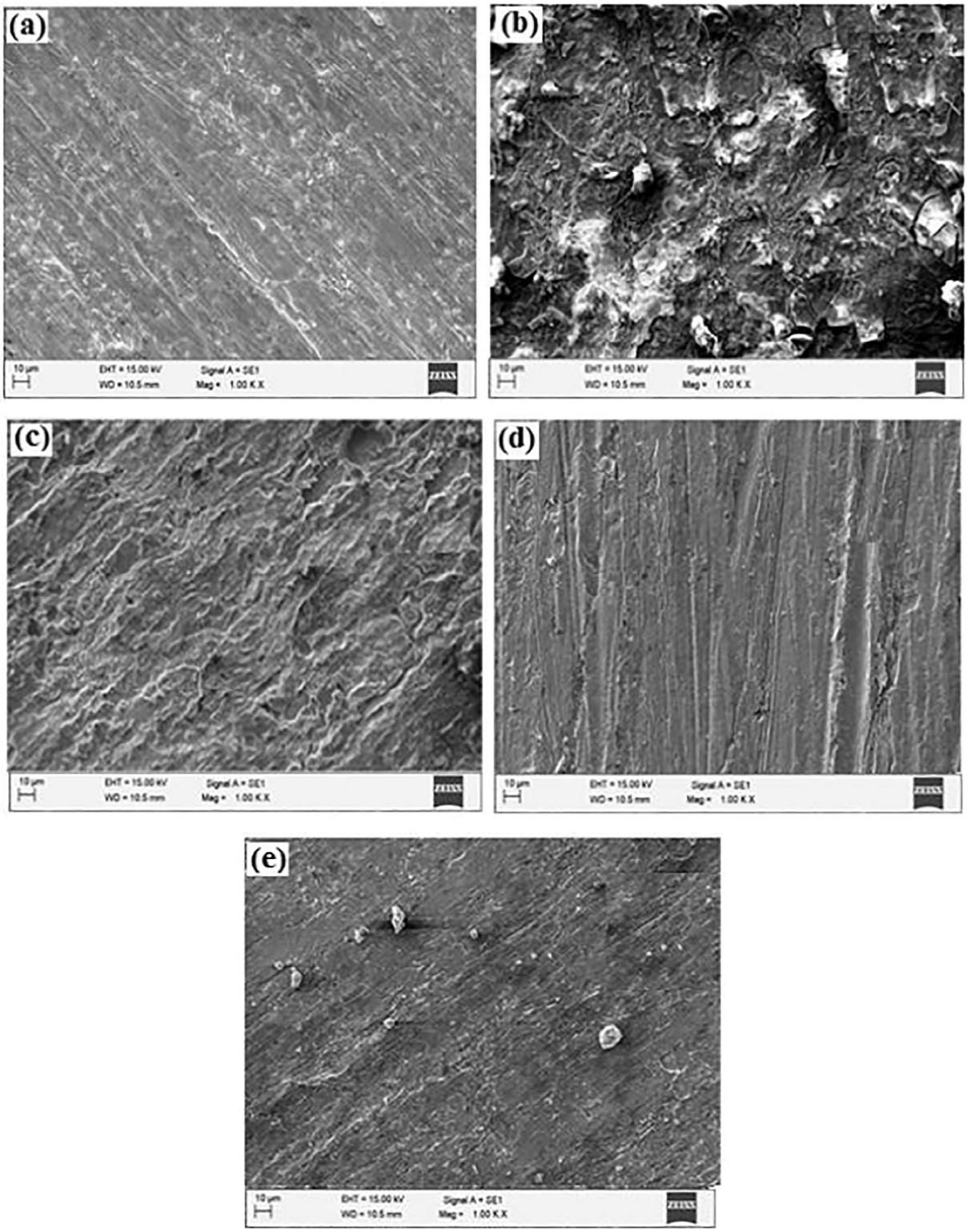


**Fig. 6.** SEM image of mild steel (a) mild steel specimen (b) mild steel immersed in 1 M HCl and mild steel immersed in 1 M HCl in the presence of (c) SGAE (d) CRRE and (e) GMLE.

In Eq. (5), $K_{ads}$ denotes a constant for adsorption-desorption phenomenon and its high value signifies the high adoptability of the plant extracts on metal surface, $C$ represents the plant extracts concentrations. The Langmuir adsorption isotherms for three tested plant extracts are shown in Fig. 5(a–c) and their respective values of $K_{ads}$ in 1 M HCl solution tabulated in Table 4. Results showed that increase in solution temperature results into decrease in $K_{ads}$ values. The dependence of the adsorption constant ($K_{ads}$) on standard free energy of adsorption ($\Delta G_{ads}$) can be presented by following relationship [39]:

$$\Delta G_{ads} = -RT\ln(55.5K\text{ads}) \tag{12}$$

In above equation, $R$ denotes the values of gas constant, quantity 55.5 represents the water concentration and $T$ is the absolute temperature. The value of $\Delta G_{ads}$ were derived using the values of $K_{ads}$

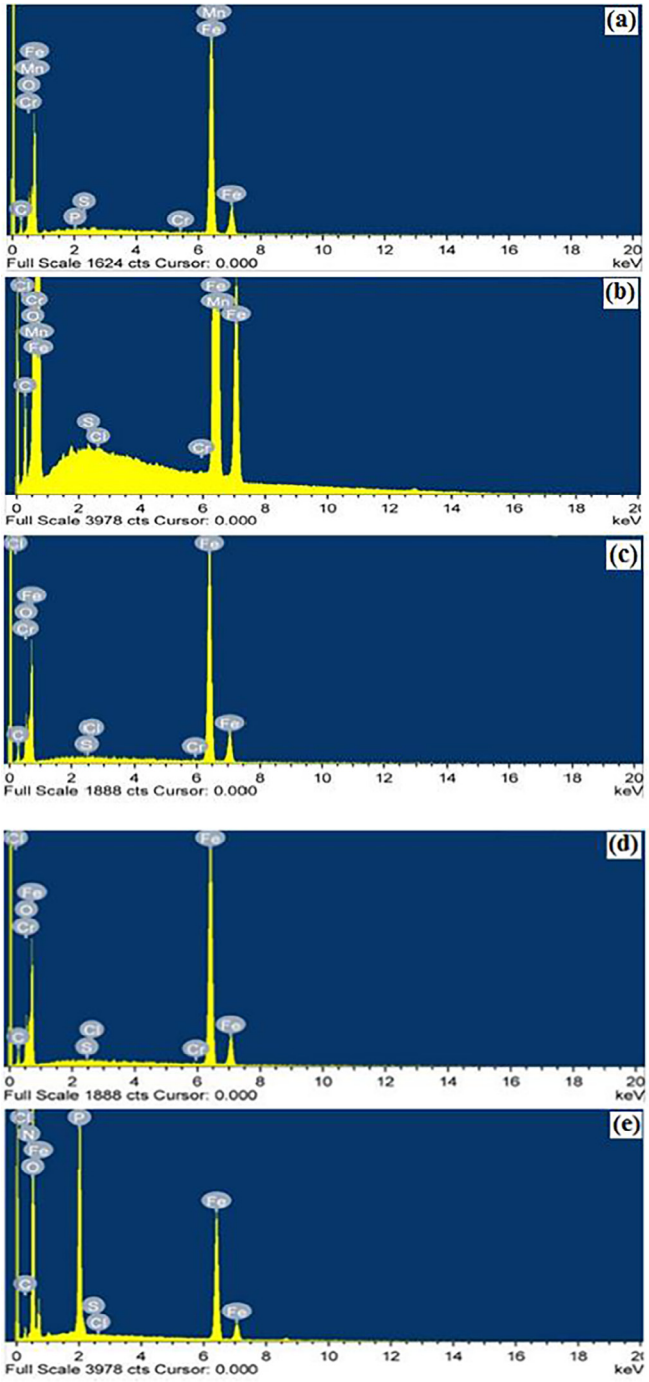


**Fig. 7.** EDS spectra of mild steel (a) mild steel specimen (b) mild steel immersed in 1 M HCl and mild steel immersed in 1 M HCl in the presence of (c) SGAE (d) CRRE and (e) GMLE.

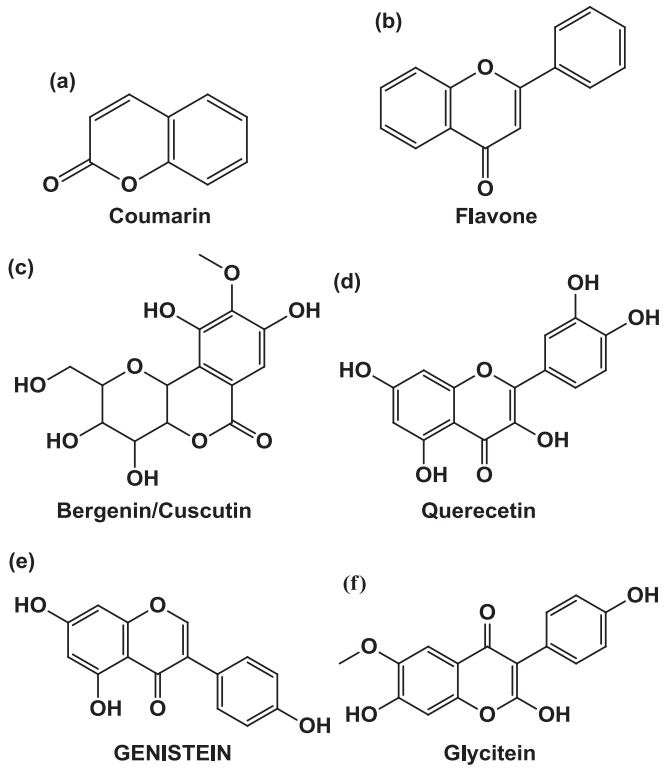


**Fig. 8.** Chemical structures of the major phytochemicals present in the extracts of the investigated plant extracts.

according to the Eq. (6) and are arranged in Table 4. It have been demonstrated that value of $\Delta G_{ads}$ near or above to $-40$ kJ/mol resulted due to chemical interactions between non-bonding and π-electrons phytochemicals and d-orbitals of the surface metallic atoms, the values of $\Delta G_{ads}$ either equal or greater than $-20$ kJ/mol resulted into physisorption between charged inhibitor and metallic surfaces [25,26,40–43]. It is manifested that in acidic solution phytochemicals/inhibitors having heteroatoms exist in their cationic forms due to their protonation and metallic surfaces become anionic due to adsorption of counter ions of aggressive acidic solutions thereby a physisorption occur between appositively charged species. The values of $\Delta G_{ads}$ in the present study for studied plant extracts are more than $-20$ kJ/mol (more positive) which argue that the phytochemicals of the plant extracts adsorbed by physisorption mechanism (Table 3).

*Surface (SEM-EDS) studies*

The surface morphologies of the metallic specimens have been demonstrated in Fig. 6(a–e). The free acidic corrosion of metallic surface (Fig. 6a) in the absence of plant extracts causes huge damage of the surface that comes out in the form of very high surface roughness. Whereas, presence of plant extracts at their 2.0 g $L^{-1}$ concentration (Fig. 6c–e) resulted into great enhancement in the surface morphology

**Table 5**
Percentage atomic contents of elements obtained from EDS spectra of mild steel in the absence and presence of inhibitors in 1 M HCl.

| Medium | Elemental composition (%) | | | | | | | | |
|---|---|---|---|---|---|---|---|---|---|
| | Fe(%) | C(%) | O(%) | P(%) | S(%) | Cr(%) | Mn(%) | N(%) | Cl(%) |
| MS | 98.66 | 0.25 | 0.06 | 0.02 | 0.05 | 0.49 | 0.47 | – | – |
| MS + HCl | 82.32 | 1.43 | 7.98 | – | 0.06 | 0.21 | 0.24 | – | 7.76 |
| MS + GMLE | 86.72 | 6.64 | 5.96 | – | 0.04 | 0.31 | – | – | 0.33 |
| MS + CRRE | 84.04 | 8.31 | 7.11 | – | 0.02 | 0.09 | – | – | 0.43 |
| MS + SGAE | 85.23 | 7.96 | 5.88 | 0.02 | 0.04 | – | – | 0.16 | 0.71 |

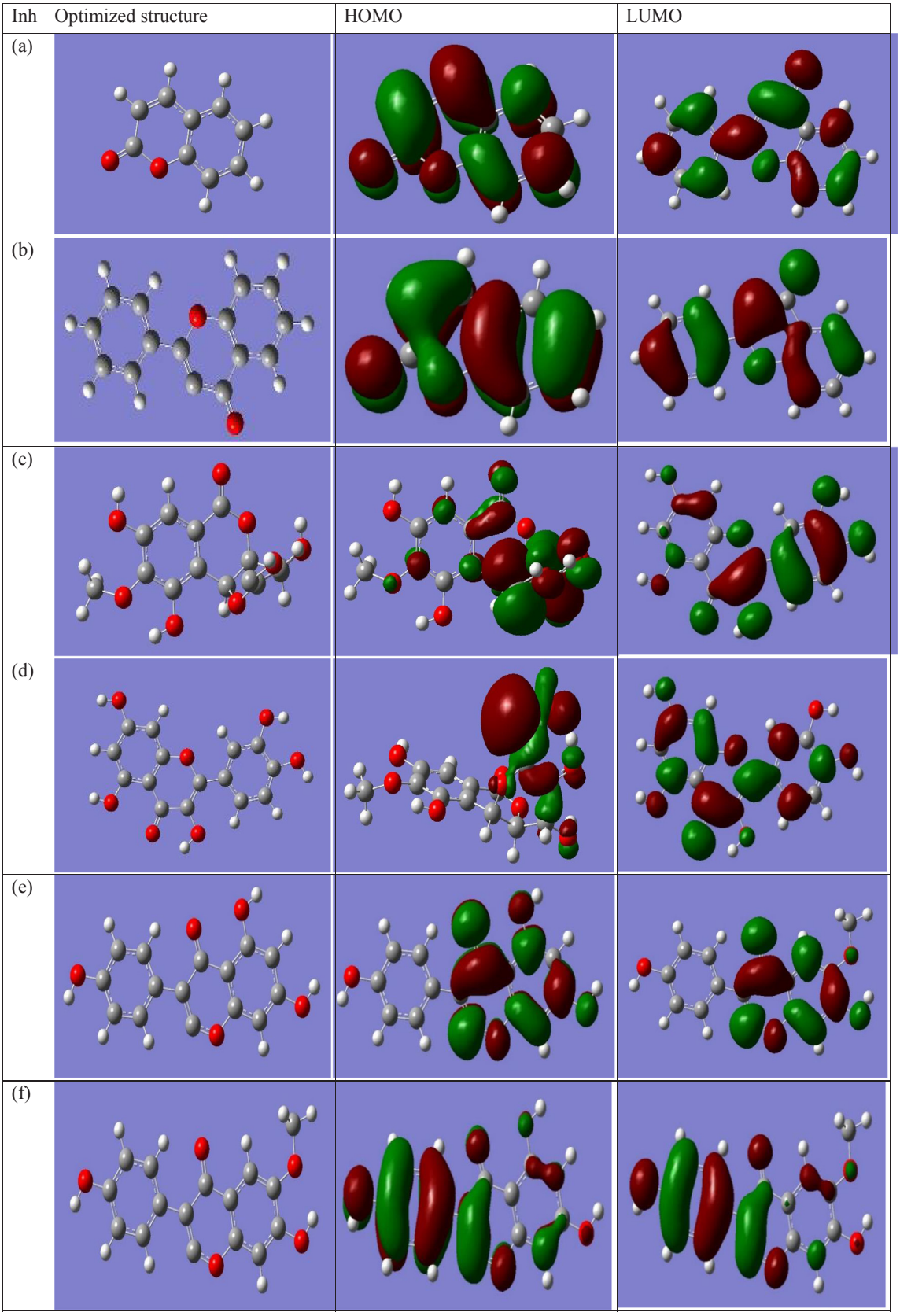


**Fig. 9.** Frontier molecular orbital pictures of major phytochemicals present in the extracts undertaken in present investigation.

(smoothness). The substantial smoothness in the surface morphologies of the plant extracts inhibited specimens it attributed due to the adsorption of the phytochemicals/phyto-constituents over the surface which isolates the metals from aggressive medium. The order of surface smoothness follows the effectiveness of the plant extracts therefore SEM analysis provides good support to the electrochemical and gravimetric

**Table 6**
Quantum chemical parameters for phytochemicals present in extracts.

| Phytochemicals | $E_{HOMO}$ (eV) | $E_{LUMO}$ (eV) | $\Delta E$ (eV) | χ | η | σ | *IE* | *EA* | $\Delta N_{110}$ | μ (Debye) |
|---|---|---|---|---|---|---|---|---|---|---|
| Coumarin | −2.186 | −2.059 | 0.126 | 2.123 | 0.063 | 15.860 | 2.186 | 2.059 | 21.389 | 5.4290 |
| Flavones | −2.286 | −2.039 | 0.247 | 2.163 | 0.124 | 8.084 | 2.286 | 2.039 | 10.741 | 3.8579 |
| Bergenin | −2.282 | −2.140 | 0.142 | 2.211 | 0.071 | 14.084 | 2.282 | 2.140 | 18.371 | 5.6170 |
| Quercetin | −2.251 | −2.215 | 0.037 | 2.233 | 0.018 | 54.200 | 2.251 | 2.215 | 70.107 | 2.5859 |
| Genistein | −2.286 | −2.093 | 0.193 | 2.189 | 0.096 | 10.341 | 2.286 | 2.093 | 13.600 | 5.0586 |
| Glycitein | −2.207 | −2.146 | 0.061 | 2.177 | 0.030 | 32.626 | 2.207 | 2.146 | 43.119 | 2.7588 |

studies. This finding suggests that phytochemicals have strong tendency to adsorb and protect surface from corrosion. It has been reported that change in the surface morphology in acidic solution is attributed to the collections of several by-products of corrosion such as FeOOH, $Fe_3O_4$, $FeO{\cdot}nH_2O$ and $FeCl_2{\cdot}nH_2O$ on the surface [33].

The surface elemental composition was studied using EDS method for uninhibited and inhibited by plant extracts metallic surfaces. The EDS spectra are shown in Fig. 7(a–e) and their composition are presented in Table 5. EDS spectra of the inhibited by plant extracts and uninhabited showed the presence of several elements which is attributed to their presence on the surface. This finding again support the adsorption mechanism of corrosion inhibition by plant extracts.

*DFT study*

It important to mention that BPLE extract mainly contains coumarin and flavone as major phytochemicals, CRRE extract mainly contains bergenin and quercetin as major phytochemicals and GMLE extract mainly contains genistein and glycitein as main phytoconstituents. Therefore, in the present study DFT study has been carried out on these phytochemicals. The chemical structures (Fig. 8), optimized, highest occupied and lowest unoccupied frontier molecular pictures of these phytochemicals are shown in Fig. 9 and several computed DFT parameters are presented in Table 6. Obviously, A high value of $E_{HOMO}$ and Low value of $E_{LUMO}$ associated with high electron sharing ability and thereby by high protection ability and vice versa [44,45]. A low value of $\Delta E$ associated with high chemical reactivity and high inhibition effectiveness. A molecule with high value of electronegativity, high value of hardness and low value of softness is associated with low chemical reactivity and inhibition efficiency as compared to the molecule having low value of electronegativity, hardness and high value of softness. Ionization energy (*IE*) and electron affinity (*EA*) cab be regarded as negative of $E_{HOMO}$ and $E_{LUMO}$, respectively. Fraction of electron transfer ($\Delta N$) is the total amount of electrons that have to be transferred from inhibitor molecules to the metallic d-orbitals. Generally, its high value is associated with high chemical reactivity and high protection ability. It is significant to mention that an inhibitor/ phytochemical with high value of dipole moment is more polarizable as compared to the molecule having less value of dipole moment. The concept of polarizability is more significant when inhibitor comes to the metallic surface and undergoes polarization. A more polarizable molecule will cover larger surface area and therefore will acts as better corrosion inhibitor as compared to the less polarizable molecule

From the results presented in Table 6 it can be see that the coumarin, flavone, bergenin, quercetin, genistein and glycitein are associated with relatively high values of $E_{HOMO}$ which imply that these phytochemicals have strong electron donating abilities [46–48]. Meanwhile, their lower values of $E_{LUMO}$ suggest that they are also very good electron acceptors. On the basis of this observations it can be predicted as all phytochemicals and good electrons donor as well as acceptors and thereby they generally offer strong metal-inhibitors bondings that come out in the form of the high protection ability of the extracts. Similarly, relatively lower values of $\Delta E$, electronegativity and hardness of these phytochemicals suggested that they are very reactive and preferably form meta-inhibitor bonding ones they come in contact with the metallic surface [49–51]. Their high value of softness and fraction of electron transfer also suggest that these phytochemicals are highly reactive and act as good corrosion inhibitors for mild steel corrosion in acidic medium. The inhibitory effect of the extract biomolecules can be attributed to the adsorption of their parallel to the surface of the metal. These molecules are attributed to the presence of more than one active centre to adsorb the metal surface. These active centers are conjugated double bonds of aromatic rings in addition to oxygen atoms in their chemical structures.

## Conclusion

Present study showed that examined plant extracts exhibits good inhibition performance toward mild steel corrosion in acidic 1 M HCl solution and their performance increases with increase in plant extracts concentration. All plant extracts showed maximum efficiency at 2.0 g $L^{-1}$ concentration. Polarization measurements showed that they behaved as mixed type corrosion inhibitors. A good correlation between surface, weight loss and electrochemical studies were observed. The inhibition efficiencies of SGAE, CRRE and GMLE follow the same order with under electrochemical, weight loss and surface measurements. Among tested plant extracts, GMLE showed the best protection ability towards mild steel corrosion. EIS study revealed that all plant extracts inhibits corrosion by adsorbing at metal (mild steel)-electrolyte (1 M HCl) interfaces and their adsorption obeyed the Langmuir isotherm. The increased values of charge transfer resistances were observed in presence of tested plant extracts which support their adsorption mechanism of inhibition which was further supported by SEM-EDS analyses.

## Acknowledgements

Chandrabhan Verma, thankfully acknowledges the North-West University (Mafikeng Campus) South Africa for providing financial support under the postdoctoral fellowship scheme.

## References

[1] Yadav M, Sinha RR, Kumar S. Corrosion inhibition effect of spiropyrimidinethiones on mild steel in 15% HCl solution: insight from electrochemical and quantum studies. RSC Adv 2015;5:70832–48.
[2] Verma C, Quraishi MA, Singh A. 2-Aminobenzene-1,3-dicarbonitriles as green corrosion inhibitor for mild steel in 1 M HCl: electrochemical, thermodynamic, surface and quantum chemical investigation. J Taiwan Inst Chem Eng 2015;49:229–39.
[3] Roy P, Maji T, Dey S. Adsorption behaviour of gluten hydrolysate on mild steel in 1 M HCl and its role as a green corrosion inhibitor. RSC Adv 2015;5:61170–8.
[4] Alkhathlan HZ, Khan M, Abdullah MMS. Anticorrosive assay-guided isolation of active phytoconstituents from *Anthemis pseudocotula* extracts and a detailed study of their effects on the corrosion of mild steel in acidic media. RSC Adv 2015;5:54283–92.
[5] Kalaiselvi P, Chellammal S, Palanichamy S. *Artemisia pallens* as corrosion inhibitor for mild steel in HCl medium. Mater Chem Phys 2010;120:643–8.
[6] Umoren SA, Solomon MM, Eduok UM. Inhibition of mild steel corrosion in $H_2SO_4$ solution by coconut coir dust extract obtained from different solvent systems and synergistic effect of iodide ions: Ethanol and acetone extracts. J Environ Chem Eng 2014;2:1048–60.
[7] Li X, Deng S, Fu H. Inhibition of the corrosion of steel in HCl, $H_2SO_4$ solutions by

bamboo leaf extract. Corros Sci 2012;62:163–75.
[8] Khadraoui A, Khelifa A, Hamitouche H. Inhibitive effect by extract of *Mentha rotundifolia* leaves on the corrosion of steel in 1 M HCl solution. Res Chem Intermed 2013;40:961–72.
[9] Ramde T, Rossi S, Zanella C. Inhibition of the Cu65/Zn35 brass corrosion by natural extract of *Camellia sinensis*. Appl Surf Sci 2014;307:209–16.
[10] Kamboj A, Saluja AK. *Bryophyllum pinnatum* (Lam.) Kurz.: phytochemical and pharmacological profile: a review. Pharmacognosy Rev 2009;3:364–74.
[11] Nwadinigwe AO. Antimicrobial activities of methanol and aqueous extracts of the stem of *Bryophyllum pinnatum* Kurz (Crassulaceae). Afr J Biotechnol 2011;10:16342–6.
[12] Cruz EA, Silva SAG, Muzitano MF, Silva PMR, Costa SS, Bergmann BR. Immuno modulatory pre-treatment with Kalanchoe pinnata extract and its quercitrin flavonoid effectively protects mice against fatal anaphylactic shock. Int Immunopharmacol 2008;8:1616–21.
[13] Adinike K, Eretan OB. Purification and partial characterization of lectin from the fresh leaves of *Kalanchoe crenata*. J Cell Biol Mol Sci 2004;37:229–33.
[14] Okwu DE, Josiah C. Evaluation of the chemical composition of two Nigerian medicinal plants. Afr J Biotechnol 2006;5(4):357–61.
[15] Gaind K, Gupta R. Alkanes, alkanols, triterpenes, and sterols of *Kalanchoe Pinnata*. Phytochemistry 1972;11:1500–2.
[16] Pal S, Sen T, Chaudhari Nag AK. Neuropsycho pharmacological profile of the methanolic fraction of Bryophyllum Pinnatum leaf extract. J Pharm Pharmacol 1999;51:313–8.
[17] Ingram D, Sanders K, Kolybaba M, Lopez D. Case-control study of phyto-oestrogens and breast cancer. Lancet 1997;350:990–4.
[18] Adlercreutz H, Hamalainen E, Gorbach S, Goldin B. Dietary phytoestrogens and the menopause in Japan. Lancet 1992;339:1233.
[19] Van de Laar FA, Lucassen PL, Akkermans RP, Van de Lisdonk EH, Rutten GE, Van Weel C. A glucosidase inhibitors for patients with type 2 diabetes. Diabetes Care 2005;28:116–75.
[20] Heung JY, Lee JH, Marcus J, Long C, Lee JW, Kim YS, et al. The most abundant polyphenol of soy leaves, coumestrol, displays potent a-glucosidase inhibitory activity. Food Chem 2011;126:1057–63.
[21] Donnapee S, Li J, Yang X, Ge A, Donkor PO, Gao X, Chang Y. Cuscuta chinensis Lam.: a systematic review on ethnopharmacology, phytochemistry and pharmacology of an important traditional herbal medicine. J Ethnopharmacol 2014;157:292–308.
[22] Wang Z, Fang JN, Ge DL, Li XY. Chemical characterization and immunological activities of an acidic polysaccharide isolated from the seeds of Cuscuta chinensis Lam". Acta Pharmacol Sin 2003;21:1136–40.
[23] Ji G, Anjum S, Sundaram S. *Musa paradisica* peel extract as green corrosion inhibitor for mild steel in HCl solution. Corros Sci 2015;90:107–17.
[24] Gunasekaran G, Chauhan LR. Eco friendly inhibitor for corrosion inhibition of mild steel in phosphoric acid medium. Electrochim Acta 2004;49:4387–95.
[25] Raja PB, Qureshi AK, Rahim AA, et al. Indole alkaloids of Alstonia angustifolia var. latifolia as green inhibitor for mild steel corrosion in 1 M HCl media. JMEPEG 2013;22:1072–8.
[26] Raja PB, Sethuraman MG. Inhibitive effect of black pepper extract on the sulphuric acid corrosion of mild steel. Mater Lett 2013;32:2977–9.
[27] Korde R, Verma CB, Ebenso EE, et al. Electrochemical and thermo dynamical investigation of 5-ethyl-4-(4-methoxyphenyl)-6-methyl-2-thioxo-1,2,3,4-tetrahydropyrimidine-5-carboxylate on corrosion inhibition behavior of aluminium in 1 M hydrochloric acid medium. Int J Electrochem Sci 2015;10:1081–93.
[28] Verma C, Haque J, Ebenso EE, Quraishi MA. Melamine derivatives as effective corrosion inhibitors for mild steel in acidic solution: chemical, electrochemical, surface and DFT studies. Results Phys 2018;9:100–12.
[29] Ferreira ES, Giancomlli C, Giacomlli FC. Evaluation of the inhibitor effect of L-ascorbic acid on the corrosion of mild steel. Mater Chem Phys 2004;83:129–34.
[30] Soltani N, Behpour M, Oguzie EE, et al. Pyrimidine-2-thione derivatives as corrosion inhibitors for mild steel in acidic environments. RSC Adv 2015;5:11145–62.
[31] Kesavan D, Tamizh MM, Gopiraman M. physicochemical studies of 4-substituted *N*-(2-mercaptophenyl)-salicylideneimines: corrosion inhibition of mild steel in an acid medium. J Surfactants Deterg 2012;15:567–76.
[32] Verma C, Lgaz H, Verma DK, Ebenso EE, Bahadur I, Quraishi MA. Molecular dynamics and Monte Carlo simulations as powerful tools for study of interfacial adsorption behavior of corrosion inhibitors in aqueous phase: a review. J Mol Liq 2018;260:99–120.
[33] Mayakrishnan G, Nagamani S, Devnarayan K. Chemical and physical interactions of 1-benzoyl-3,3-disubstituted thiourea derivatives on mild steel surface: corrosion inhibition in acidic media. Ind Eng Chem Res 2012;51:7910–22.
[34] Verma DK, Khan F. Corrosion inhibition of mild steel in hydrochloric acid using extract of glycine max leaves. Res Chem Intermed 2016;42:3489–506.
[35] Solomon MM, Umoren SA, Udousoro II. Inhibitive and adsorption behaviour of carboxymethyl cellulose on mild steel corrosion in sulphuric acid solution. Corros Sci 2010;52:1317–25.
[36] Shahi G, Verma CB, Ebenso EE. Thermodynamic and electrochemical investigation of (9-[(R)2[[bis[[(isopropoxycarbonyl)oxy]methoxy]phosphinyl]methoxy]propyl] adenine fumarate) as green corrosion inhibitor for mild steel in 1 M HCl. Int J Electrochem Sci 2015;10:1102–16.
[37] Singh AK, Khan S, Singh A. Inhibitive effect of chloroquine towards corrosion of mild steel in hydrochloric acid solution. Res Chem Intermed 2013;39:1191–208.
[38] Solmazm R. Investigation of corrosion inhibition mechanism and stability of Vitamin B1 on mild steel in 0.5 M HCl solution. Corros Sci 2014;81:75–84.
[39] Gobara M, Baraka A, Zaghloul B. Inhibition of mild steel corrosion in sulfuric acid solution using collagen. Res Chem Intermed 2014;41:7245–61.
[40] Haque J, Verma C, Srivastava V, Quraishia MA, Ebenso EE. Experimental and quantum chemical studies of functionalized tetrahydropyridines as corrosion inhibitors for mild steel in 1 M hydrochloric acid. Results Phys 2018;9:1481–93.
[41] Sudheer, Quraishi MA. The corrosion inhibition effect of aryl pyrazolo pyridines on copper in hydrochloric acid system: computational and electrochemical studies. RSC Adv 2015;5:41923–33.
[42] Verma C, Olasunkanmi LO, Ebenso EE, Quraishi MA. Adsorption characteristics of green 5-arylaminomethylene pyrimidine2,4,6-triones on mild steel surface in acidic medium: experimental and computational approach. Results Phys 2018;8:657–70.
[43] Vishwakarma S, Mourya P, Chaubey N. *Strychnos nuxvomica*, *Piper longum* and *Mucuna pruriens* seed extracts as eco-friendly corrosion inhibitors for copper in nitric acid. RSC Adv 2016;6:95644–55.
[44] Verma C, Quraishi MA, Ebenso EE, Bahadur I. A green and sustainable approach for mild steel acidic corrosion inhibition using leaves extract: experimental and DFT studies. J Bio- Tribo-Corrosion 2018;4:1–12.
[45] Eddy NO, Ebenso EE. Quantum chemical studies on the inhibition potentials of some Penicillin compounds for the corrosion of mild steel in 0.1 M HCl. J Mol Model 2010;16:1291–306.
[46] Migahed MA, Elsaeed SM, Al-Sabagh AM, Khamis EA, Zaki EG. "Quantum chemical calculations, synthesis and corrosion inhibition efficiency of (2R,3R,4S,5S,6S)-N,Ndidodecyl-5-ethyl-4-hydroxy-6-(hydroxymethyl)-N-(5-hydroxypentyl)-2-(methoxymethyl)-2,3,4,5,6-pentamethyltetrahydro-3-aminium chloride on X-65 tubing in acidic solution. Res J Pharm Biol Chem Sci 2016;7:1669.
[47] Lee C, Yang W, Parr RG. Development of the Colle-Salvetti correlation-energy formula into a functional of the electron density. Phys Rev B 1988;37:785.
[48] Miehlich B, Savin A, Stoll H, Preuss H. Results obtained with the correlation energy density functionals of becke and Lee, Yang and Parr. Chem Phys Lett 1989;157:200–6.
[49] Verma C, Olasunkanmi LO, Quadri TW, El-Sayed MS, Ebenso EE. Gravimetric, electrochemical, surface morphology, DFT, and Monte Carlo simulation studies on three N–Substituted 2–Aminopyridine derivatives as corrosion inhibitors of mild steel in acidic medium. J Phys Chem C 2018;122:11870–82.
[50] Xia S, Qiu M, Yu L, Liu F, Zhao H. Molecular dynamics and density functional theory study on relationship between structure of imidazoline derivatives and inhibition performance. Corros Sci 2008;50:2021–9.
[51] Gaussian 09, Revision A.02, Frisch MJ, Trucks GW, Schlegel HB, Scuseria GE, Robb MA, Cheeseman JR, et al. Gaussian, Inc., Wallingford CT; 2009.